1979

# Smooth interpolation of large sets of scattered data

Franke, Richard; Nielson, Gregory

Monterey, California. Naval Postgraduate School

NPS-53-79-005

# NAVAL POSTGRADUATE SCHOOL

## Monterey, California

SMOOTH INTERPOLATION OF LARGE SETS

OF SCATTERED DATA

Richard Franke
Gregory Nielson

Technical Report for Period Jan 79 - Mar 79



proved for public release; distribution unlimited

epared for: Chief of Naval Research
Arlington, VA 22217

NAVAL POSTGRADUATE SCHOOL
Monterey, California

Rear Admiral Tyler F. Dedman
Superintendent

Jack Borsting
Provost

The work reported herein was supported in part by the Foundation Research Program of the Naval Postgraduate School with funds provided by the Chief of Naval Research, and in part by the Office of Naval Research under contract NR 044-443.



This report was prepared by:

UNCLASSIFIED

SECURITY CLASSIFICATION OF THIS PAGE *(When Data Entered)*

| REPORT DOCUMENTATION PAGE | | READ INSTRUCTIONS BEFORE COMPLETING FORM |
|---|---|---|
| 1. REPORT NUMBER<br>NPS-53-79-005 | 2. GOVT ACCESSION NO. | 3. RECIPIENT'S CATALOG NUMBER |
| 4. TITLE *(and Subtitle)*<br>Smooth Interpolation of Large Sets of Scattered Data | | 5. TYPE OF REPORT & PERIOD COVERED<br>Technical Report<br>Jan 1979-Mar 1979<br>6. PERFORMING ORG. REPORT NUMBER |
| 7. AUTHOR(s)<br>Richard Franke<br>Greg Nielson | | 8. CONTRACT OR GRANT NUMBER(s) |
| 9. PERFORMING ORGANIZATION NAME AND ADDRESS<br>Foundation Research Program<br>Naval Postgraduate School<br>Monterey, CA 93940 | | 10. PROGRAM ELEMENT, PROJECT, TASK AREA & WORK UNIT NUMBERS<br>61152N, RR 000-01-01<br>N0001479WR90027 |
| 11. CONTROLLING OFFICE NAME AND ADDRESS<br>Chief of Naval Research<br>Arlington, VA 22217 | | 12. REPORT DATE<br>9 March 1979<br>13. NUMBER OF PAGES<br>36 |
| 14. MONITORING AGENCY NAME & ADDRESS*(if different from Controlling Office)* | | 15. SECURITY CLASS. *(of this report)*<br>Unclassified<br>15a. DECLASSIFICATION/DOWNGRADING SCHEDULE |

16. DISTRIBUTION STATEMENT *(of this Report)*

Approved for public release; distribution unlimited

17. DISTRIBUTION STATEMENT *(of the abstract entered in Block 20, if different from Report)*

18. SUPPLEMENTARY NOTES

19. KEY WORDS *(Continue on reverse side if necessary and identify by block number)*

Scattered data interpolation
Interpolation
Smooth interpolation
Bivariate interpolation
Multivariate approximation

20. ABSTRACT *(Continue on reverse side if necessary and identify by block number)*

Methods for solving the following data fitting problems are discussed: Given the data $(x_i, y_i, f_i)$, $i = 1,\ldots,N$ construct a smooth bivariate function S with the property that $S(x_i, y_i) = f_i$, $i = 1,\ldots,N$. Because the desire to fit this type of data is encountered frequently in many areas of scientific applica-

DD FORM 1 JAN 73 1473 EDITION OF 1 NOV 65 IS OBSOLETE
S/N 0102-014-6601 |

UNCLASSIFIED

SECURITY CLASSIFICATION OF THIS PAGE *(When Data Entered)*

this problem was undertaken. Several aspects, such as computational efficiency, fitting characteristics and ease of implementation, were analyzed and compared. Within the context of a general purpose method for large sets of data, two of these methods emerged as being generally superior to the others. It is the purpose of this paper to describe these two methods and present examples illustrating their use and application. FORTRAN programs which implement these methods are available upon request.

## 1. Introduction

The purpose of this paper is to describe two methods for constructing smooth bivariate functions which take on given values at scattered points in the plane. Given the data $(x_i, y_i, f_i)$, $i = 1,\ldots,N$, both of these schemes define a smooth bivariate interpolant $S$ with the property that $S(x_i,y_i) = f_i$, $i = 1,\ldots,N$.

In the past several years a number of methods have been proposed (e.g., [1], [3], [6], [7], [8], and [11]), and two survey papers, [2] and [10], have dealt extensively with this topic. The problem of constructing smooth approximations based upon scattered data is encountered frequently in many areas of scientific applications. Common examples are: meteorological information such as rainfall and solar insolation, geographical information such as elevations, geological information such as depths of underground formations, and engineering data such as stress values obtained by finite element analysis. A somewhat less obvious example is given in [10] where it is described how human heart potential is measured at irregularly spaced points as an aid in diagnosing abnormal heart conditions.

Since a number of methods are available for this important problem, a project was undertaken to test and compare as many methods as possible [4]. While the project included both global methods (meaning that $S(x,y)$ is dependent on all data points regardless of their distance from

(x,y)) and local methods (S(x,y) does not depend on data points more than a certain distance from (x,y)), for large sets of data it is necessary to use local methods. During the course of developing and testing variations of previously published schemes we have discovered two which appear to be preferable as general purpose methods. While neither of these methods have appeared in the literature, they are both modifications of previously described techniques. In Section 2, we describe the basic method from which both of our methods derive. In Section 3, we describe the details of the two modifications and in Section 4 we show the results of applying these methods to certain test problems. In Section 5, we discuss some generalizations and ways to fine tune the schemes to suit the particular needs of a user.

## 2. Inverse Distance Weighted Least Squares Interpolation

It is convenient to consider the data as coming from an underlying function $f$ and to view the interpolation process as an operator applied to this function. That is, $f_i = f(x_i,y_i)$, $i = 1,\ldots,N$ and $S(x,y) = P[f](x,y)$. Let $\rho_i(x,y)$ denote a function with certain properties of a distance function. In particular, we assume that $\rho_i(x_i,y_i) = 0$ and that $1/\rho_i(x_i,y_i)$ is a nonnegative decreasing function as $(x,y)$ "gets further" from $(x_i,y_i)$. For example, the usual Euclidean distance, $d_i(x,y) = \sqrt{(x - x_i)^2 + (y - y_i)^2}$ is one possibility for $\rho_i$. We denote by $\phi_j$, $j = 1,\ldots,m$ a set of basis functions to be used for a least squares approximation.

McLain [7] was the first to consider a family of inverse distance weighted least squares approximations. The general form of these interpolants is

$$(2.1) \qquad P[f](x,y) = \sum_{j=1}^{m} \bar{a}_j(x,y)\phi_j(x,y)$$

where $\bar{a}_j(x,y)$, $j = 1,\ldots,m$ represents the solution of

$$(2.2) \qquad \min_{a_1,\ldots,a_m} \sum_{i=1}^{N} \left[ \frac{a_1\phi_1(x_i,y_i) + \ldots + a_m\phi_m(x_i,y_i) - f_i}{\rho_i(x,y)} \right]^2$$

for given $(x,y)$. McLain gave results of a number of tests for several choices of basis functions, $\phi_j$, and distance functions, $\rho_i$. The $\phi_j$ consisted of the low order monomials, $x^k y^\ell$, and $\rho_i$ was taken as $d_i$, $d_i^2$, or $d_i e^{\alpha d_i^2}$. The higher power of $d_i$ and the exponential are motivated by the desire to place less importance on distant data than would be accomplished by $d_i$ alone.

The function (2.1) is not defined at any data point, $(x_i,y_i)$, by the above definition. Because the weight for the best least squares approximation $1/\rho_i^2(x,y) \longrightarrow \infty$ as $(x,y) \longrightarrow (x_i,y_i)$ it is clear that $P[f](x,y) \longrightarrow f_i$ as $(x,y) \longrightarrow (x_i,y_i)$, else the sum of the squared errors would be unbounded. Thus we obtain a continuous approximation if we define $P[f](x_i,y_i) = f_i$, $i = 1,\ldots,N$. McLain asserts that the interpolants are infinitely differentiable, and upon the assumption of non-singularity of the coefficient matrix for the normal equations

obtained from (2.2), this readily follows.

McLain singled out the case of the bivariate quadratic, $P[f](x,y) = \bar{a}_1 + \bar{a}_2 x + \bar{a}_3 y + \bar{a}_4 x^2 + \bar{a}_5 xy + \bar{a}_6 y^2$, with weight function $\rho_i = d_i e^{\alpha d_i^2}$ as working well for a variety of problems in the sense that small deviations from certain test functions were observed. Additional experimentation [3] has confirmed this, but even so this method has two serious drawbacks: (1) The computational effort required is large since each evaluation requires the solution of a least squares problem, and (2) the method is global, that is, the interpolant depends on all data points regardless of how far away these points are from the point at which the interpolant is being evaluated.

Both of the methods we propose can be viewed as modifications of the above inverse distance weighted least squares interpolant in that they consist of replacing $\bar{a}_j(x,y)$ with an approximation $A[\bar{a}_j](x,y)$ which is computationally more tractable than $\bar{a}_j(x,y)$ itself. We note that as long as

$$A[\bar{a}_j](x_i,y_i) = \bar{a}_j(x_i,y_i), \quad i = 1,\ldots,N,$$

the operator

$$Q[f](x,y) = \sum_{j=1}^{m} A[\bar{a}_j](x,y)\phi_j(x,y)$$

will maintain the interpolatory properties of $P[f]$. The type

of approximation we use for $\bar{a}_j$, $j = 1,\ldots,m$ is of the form

$$A[\bar{a}_j](x,y) = \sum_{i=1}^{N} \bar{a}_j(x_i,y_i)\, W_i(x,y)$$

where

$$W_i(x_j,y_j) = \delta_{ij},\ i,\ j = 1,\ldots,N. \tag{2.3}$$

Therefore, we may rewrite the above expression for Q as

$$Q[f](x,y) = \sum_{i=1}^{N} W_i(x,y) Q_i(x,y) \tag{2.4}$$

where $Q_i(x,y) = \sum_{j=1}^{m} \bar{a}_j(x_i,y_i)\phi_j(x,y)$ is the inverse distance weighted least squares fit at the point $(x_i,y_i)$.

We refer to the functions $Q_i$, $i = 1,\ldots,N$ as the nodal functions since they are associated with the nodes $(x_i,y_i)$, $i = 1,\ldots,N$, respectively. We note that $Q_i(x_i,y_i) = f_i$, $i = 1,\ldots,N$, and that $Q_i(x,y)$ is a local approximation (near $(x_i,y_i)$) to $f(x,y)$, and as such may be expected to mimic the shape of $f(x,y)$ provided distant points do not influence $Q_i(x,y)$ too much.

In order for the interpolant Q[f] to maintain the local shape characteristics of the nodal functions we will require certain properties for the $W_i$ in addition to (2.3). Specifically, to preserve

$$\frac{\partial Q[f]}{\partial x}(x_i,y_i) = \frac{\partial Q_i}{\partial x}(x_i,y_i)$$

and

$$\frac{\partial Q[f]}{\partial y}(x_i,y_i) = \frac{\partial Q_i}{\partial y}(x_i,y_i), \; i = 1,\ldots,N \; ;$$

we require that

$$\frac{\partial W_i}{\partial x}(x_j,y_j) = \frac{\partial W_i}{\partial y}(x_j,y_j) = 0, \; i, \; j = 1,\ldots,N. \tag{2.5}$$

For our two methods, we also propose the use of bivariate quadratics for $Q_i(x,y)$, $i = 1,\ldots,N$. Thus, if $f$ itself is a quadratic function, the function $Q_i$ will be identical to $f$, i.e., $Q_i(x,y) = f(x,y)$, $i = 1,\ldots,N$.
Therefore

$$Q[f](x,y) = \sum_{i=1}^{N} W_i(x,y)Q_i(x,y) = f(x,y) \sum_{i=1}^{N} W_i(x,y)$$

whenever $f$ is a quadratic function. In order to obtain quadratic precision of the modified interpolant $Q[f]$, we add the additional requirement that

$$\sum_{i=1}^{N} W_i(x,y) \equiv 1. \tag{2.6}$$

The choice of the distance function to be used in (2.2) when calculating the nodal functions was made on the basis

of extensive numerical testing [4]. Franke and Little [2, p. 112] proposed

$$(2.7) \qquad \frac{1}{\rho_i} = \frac{(R_i - d_i)_+}{R_i d_i}, \quad (R_i - d_i)_+ = \begin{cases} R_i - d_i, & R_i - d_i \geq 0 \\ 0 & R_i - d_i < 0, \end{cases}$$

and for appropriate choice of the values $R_i$, this works well. We recall that $Q_k$ is the solution of the inverse distance weighted least squares problem at $(x,y) = (x_k,y_k)$. Discussion of the $Q_k$ is simplified (as is the actual computation) by assuming that

$$Q_k(x,y) = f_k + \bar{a}_{k2}(x-x_k) + \bar{a}_{k3}(y-y_k) + \bar{a}_{k4}(x-x_k)^2 +$$

$$\bar{a}_{k5}(x-x_k)(y-y_k) + \bar{a}_{k6}(y-y_k)^2 .$$

We then seek the solution of

$$\underset{a_{k2},\ldots,a_{k6}}{\text{Min}} \sum_{\substack{i=1 \\ i\neq k}}^{N} \left[ \frac{f_k + a_{k2}(x_i-x_k) + \ldots + a_{k6}(y_i-y_k)^2 - f_i}{\rho_i(x_k,y_k)} \right]^2 .$$

If $\frac{1}{\rho_i}$ is given by (2.7), then whenever $d_i(x_k,y_k) > R_i$, the point $(x_i,y_i,f_i)$ has no influence since the corresponding term in the sum is zero. Thus $Q_k$ depends only on "nearby" points and is therefore a local approximation to $f$. If we now use weight functions $W_k$ which are nonzero only in some neighborhood of $(x_k,y_k)$ we will obtain a local interpolant.

The proper choice of the "radii of influence", $R_i$, is critical to the success of the method, and we will discuss

this in the context of our first method in the next section, as well as in Section 5.

## 3. Two Methods for Interpolation To Scattered Data

Specifying the weight functions $W_i(x,y)$, $i = 1,\ldots,N$ to be used in (2.4) will define an interpolant. We have found that both of the choices we propose have very comparable fitting capabilities, but we feel that there are situations in which one or the other may be preferable, and so both are presented.

### 3.1 Method I.

This scheme is based upon a special case of the inverse distance weighted least squares interpolant given by (2.1) - (2.2). If $m = 1$ and $\phi_1(x) \equiv 1$, then (2.2) can be explicitly solved to yield

$$\bar{a}_1(x,y) = \frac{\sum_{i=1}^{N} \frac{f_i}{\rho_i^2}(x,y)}{\sum_{i=1}^{N} \frac{1}{\rho_i^2}(x,y)}$$

and so

$$P[f] = \frac{\sum_{i=1}^{N} \frac{f_i}{\rho_i^2}}{\sum_{i=1}^{N} \frac{1}{\rho_i^2}} \tag{3.1}$$

This method was first proposed by Shepard [11]. Without modification it does not have very good fitting properties. Gordon and Wixom [5] have analyzed this method and have proposed some interesting modifications. They also discuss some application areas that are well suited for this type of interpolant. The fact that Shepard's method is a special case of inverse distance weighted least squares interpolants has been pointed out by several authors, e.g. [10]. It can easily be verified that as long as $\rho_i(x_i,y_i) = 0$, the functions

$$W_i = \frac{\frac{1}{\rho_i^2}}{\sum_{k=1}^{N} \frac{1}{\rho_k^2}} \tag{3.2}$$

will satisfy the conditions of (2.3), (2.5), and (2.6). This last statement assumes that the distance functions $\rho_i$, i = 1,...,N are sufficiently smooth so that the derivatives (2.5) exist. This is certainly the case for our choice of $\rho_i$, i = 1,...,N given by (2.7).

We complete the description of our first method with a discussion of the selection of the $R_i$ involved in the definition of $\rho_i$. While the use of variable radii (i.e., $R_i \neq R_j$) adds to the flexibility of the methods, we have found that for a general purpose interpolant, the selection of these values can quite often be a nuisance which can be avoided by the use of a uniform value ($R_i = R$ for all i).

At this point we emphasize that the distance functions $\rho_i$ enters in two places: (1) definition of the nodal

functions, $Q_k$, and (2) definition of the weight functions, $W_k$. It is not necessary to use the same radius of influence for both instances, and experience has shown it is desirable to use different values, say $R = R_q$ in defining the nodal functions, and $R = R_w$ in defining the weight functions. Since $R_q$ denotes the radius of influence of the data points on the nodal functions, while $R_w$ denotes the radius of influence of the nodal functions on the interpolant $Q[f](x,y)$, it is clear we should take $R_w \leq R_q$. In order to aid the naive user in making reasonable choices of $R_q$ and $R_w$ we have found it convenient to specify values of $N_q$ and $N_w$ and to compute the radii of the influence regions according to the relationships:

$$R_q = \frac{D}{2}\sqrt{\frac{N_q}{N}}$$

(3.3)

$$R_w = \frac{D}{2}\sqrt{\frac{N_w}{N}}$$

where $D = \max_{i,j} d_i(x_j,y_j)$.

These choices of $R_q$ and $R_w$ eliminate the effects of scaling the data. The values of $N_q$ and $N_w$ can be thought of as representing the number of data points anticipated to lie in circles of radii $R_q$ and $R_w$, respectively. For somewhat uniformly distributed data, we have found that a value of $N_q = 18$ works quite well. For data that have some regions which are relatively sparsely populated and other regions where the data are comparatively dense, or for small sets ($N < 25$), it may be necessary to increase the values, since the interpolant

is defined only on the union of disks of radius $R_w$ centered at the data points $(x_i,y_i)$, $i = 1,\ldots,N$. We have also found that the use of the relationship $N_q/N_w \sim 2$ is useful. To avoid problems when fewer than five additional data points fall within a distance $R_q$ of some given $(x_i,y_i)$, we have incorporated an automatic fallback to linear nodal functions in this case. In general, we use the singular value decomposition to compute the coefficients of the nodal functions, which avoids possible nonuniqueness problems. It is not usual for either situation to occur, however.

We now summarize the description of our first method.

i) Select $N_q$ and $N_w$ in order to define

$$\frac{1}{\rho_i} = \frac{(R_q-d_i)_+}{R_q d_i}, \quad R_q = \frac{D}{2}\sqrt{\frac{N_q}{N}}$$

$$\frac{1}{\hat{\rho}_i} = \frac{(R_w-d_i)_+}{R_w d_i}, \quad R_w = \frac{D}{2}\sqrt{\frac{N_w}{N}}$$

Default values of $N_q$ and $N_w$ are 18 and 9, respectively.

ii) For $k = 1,\ldots,N$ solve the least squares problem:

$$\min_{a_{kj}, j=2,\ldots,6} \sum_{\substack{i=1 \\ i\neq k}}^{N} \frac{1}{\rho_i^2(x_k,y_k)} \Big[ f_k + a_{k2}(x_i-x_k) + a_{k3}(y_i-y_k) + a_{k4}(x_i-x_k)^2 + a_{k5}(x_i-x_k)(y_i-y_k) + a_{k6}(y_i-y_k)^2 - f_i \Big]^2$$

to yield $\bar{a}_{kj}$, $j = 2,\ldots,6$.

iii) Define

$$Q_k(x,y) = f_k + \bar{a}_{k2}(x-x_k) + \bar{a}_{k3}(y-y_k)$$
$$+ \bar{a}_{k4}(x-x_k)^2 + \bar{a}_{k5}(x-x_k)(y-y_k) + \bar{a}_{k6}(y-y_k)^2$$

and compute

$$D[f](x,y) = \frac{\sum_{k=1}^{N} \frac{Q_k(x,y)}{\hat{\rho}_k^2(x,y)}}{\sum_{k=1}^{N} \frac{1}{\hat{\rho}_k^2(x,y)}}$$

3.2 Method II.

Our second method makes use of a triangulation of the data $V_i = (x_i,y_i)$ $i = 1,\ldots,N$ in order to define the weight functions $W_i$, $i = 1,\ldots,N$. We use an algorithm which triangulates the convex hull based upon the min-max angle criterion as described by Lawson [6]. A FORTRAN program which implements this algorithm is available as part of [1]. Alternatively, if a triangulation is in existence for other purposes, it can be used.

Each $W_i$ will be a globally defined $C^1$ function with support $S_i = \bigcup_{jkl \in M_i} T_{jkl}$, where $T_{jkl}$ denotes the triangle with vertices $V_j$, $V_k$, and $V_l$ and $M_i = \{jkl: T_{jkl}$ is a triangle with vertex $V_i\}$.

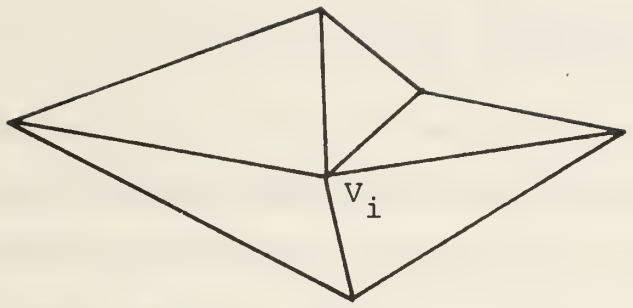


Figure 1: $S_i$

We first define $W_i$ and its first order partial derivatives on $E = \bigcup_{kj \in N_e} e_{kj}$ where $e_{kj}$ represents the edge with vertices $V_k$ and $V_j$ and $N_e = \{kj: \overline{V_k V_j}$ is an edge of the triangulation$\}$. Following this, we incorporate a blending method for triangles to extend the definition to the interior of each triangle of the triangulation. Let $e_{ij}$ be an edge contained in $S_i$ with $V_i$ as an endpoint. As a univariate function along this edge, $W_i$ must satisfy four conditions imposed by (2.3) and (2.5). Namely

$$W_i(V_i) = 1,\ W_i(V_j) = 0,$$

$$(x_j - x_i)\frac{\partial W_i}{\partial x}(V_i) + (y_j - y_i)\frac{\partial W_i}{\partial y}(V_i) = 0$$

and

$$(x_j - x_i)\frac{\partial W_i}{\partial x}(V_j) + (y_j - y_i)\frac{\partial W_i}{\partial y}(V_j) = 0.$$

These conditions can be satisfied by a cubic polynomial and so we define

$$W_i((1-t)V_i + tV_j) = (1-t)^2(2t+1),\ 0 \le t \le 1.$$

On all other edges we define $W_i$ to be zero. In order to maintain continuity of the first order derivatives across edges, it is convenient to specify the derivatives normal to an edge as a linear function along the edge. That is

$$(y_j-y_i)\frac{\partial W_i}{\partial x}((1-t)V_i + tV_j) - (x_j-x_i)\frac{\partial W_i}{\partial y}((1-t)V_i + tV_j)$$

$$= (1-t)\left[(y_j-y_i)\frac{\partial W_i}{\partial x}(V_i) - (x_j-x_i)\frac{\partial W_i}{\partial y}(V_i)\right]$$

$$+ t\left[(y_j-y_i)\frac{\partial W_i}{\partial x}(V_j) - (x_j-x_i)\frac{\partial W_i}{\partial y}(V_j)\right].$$

In light of (2.5), this means that the normal derivatives will all be identically zero. This completes the description of the edge information for $W_i$.

In order to extend the definition of $W_i$ to the interior of each triangle, we use an interpolation method [9] which will assume predescribed position and slope on the entire boundary of a triangle domain. After substituting the edge information into this triangular blending method, we find that for $(x,y) \in T_{ijk} \subset S_i$, the weight functions have the form

$$W_i(x,y) = b_i^2(3-2b_i)$$

$$(3.4) \qquad + 3\,\frac{b_i^2 b_j b_k}{b_i b_j + b_i b_k + b_j b_k}\left\{ b_j \left[ \frac{\|e_i\|^2 + \|e_k\|^2 - \|e_j\|^2}{\|e_k\|^2} \right] + b_k \left[ \frac{\|e_i\|^2 + \|e_j\|^2 - \|e_k\|^2}{\|e_j\|^2} \right] \right\} .$$

where $b_i$, $b_j$, $b_k$ are the barycentric coordinates of $(x,y)$ with respect to the triangle $T_{ijk}$ and $\|e_n\|$ $n = i, j$ or $k$ represents the length of the edge opposite $V_n$, $n = i, j$ or $k$. The barycentric (area) coordinates are given by the equations

$$(3.5) \qquad \begin{aligned} x &= b_i x_i + b_j x_j + b_k x_k \\ y &= b_i y_i + b_j y_j + b_k y_k \\ 1 &= b_i + b_j + b_k \ . \end{aligned}$$

We can now note that on an arbitrary triangle $T_{ijk}$ the only weights which are nonzero are $W_i$, $W_j$ and $W_k$. Therefore, the final interpolant is given by

$$(3.6) \qquad \begin{aligned} G[f](x,y) &= W_i(x,y)Q_i(x,y) + W_j(x,y)Q_j(x,y) \\ &\quad + W_k(x,y)Q_k(x,y) \ , \ (x,y) \in T_{ijk}. \end{aligned}$$

We also note that $W_i + W_j + W_k = 1$, so that (2.6) is satisfied. We now summarize this method.

i) Define the nodal functions $Q_k$, $k = 1,\ldots,N$ as in Method I,

ii) Form a triangulation of the points $V_i = (x_i, y_i)$, $i = 1,\ldots,N$,

iii) Given $(x,y)$ determine the vertices $V_i$, $V_j$ and $V_k$ of the triangle that contains this point and compute $G[f](x,y)$ according to (3.6) using (3.4) and (3.5).

We note that this method is very similar to that proposed by McLain [8]. Our weight functions $W_i$, $i = 1,\ldots,N$ arise in a natural manner, however, and use of the distance function given in (2.7) is an improvement since it is generally the case that shape characteristics of the nodal functions in relation to $f$ are adversely influenced when global approximations are used.

## 4. Examples

In order to illustrate the performance of the two methods, we include some examples. These examples are only a few of many upon which our conclusions are based, but are representative of the methods' approximation properties. The first group of examples utilizes ordinates from the function

$$f(x,y) = .75\text{EXP}\left[-\frac{(9x-2)^2+(9y-2)^2}{4}\right] + .75\text{EXP}\left[-\frac{(9x+1)^2}{49} - \frac{(9y+1)}{10}\right]$$

$$- .2\text{EXP}\left[-(9x-4)^2 - (9y-7)^2\right] + .5\text{EXP}\left[-\frac{(9x-7)^2+(9y-3)^2}{4}\right].$$

A perspective plot of this surface, viewed from the first quadrant at an angle of 30° from the x-axis is given in figures 3a and 4a. The function was chosen so as to present a variety of behavior in a single surface. The maximum value of the function is approximately 1.22 near the point (.22, .22), while the minimum value is approximately .004 near the point (.47, .78). Three sets of data $(x_i,y_i)$, $i = 1,\ldots,N$ were used.

Set 1: This set consists of 100 points generated by a pseudorandom number generator, one point in each subsquare

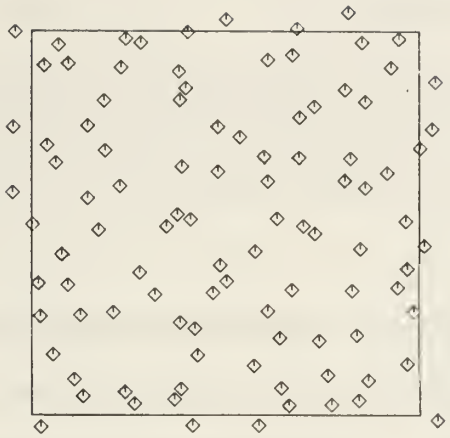

(a) Data Set 1

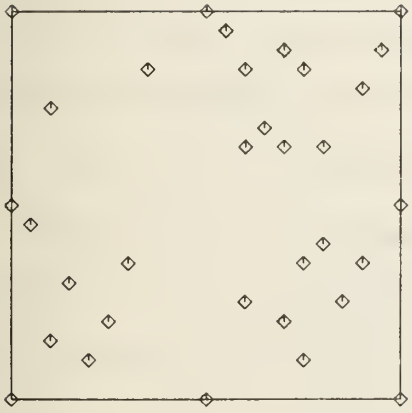

(b) Data Set 2

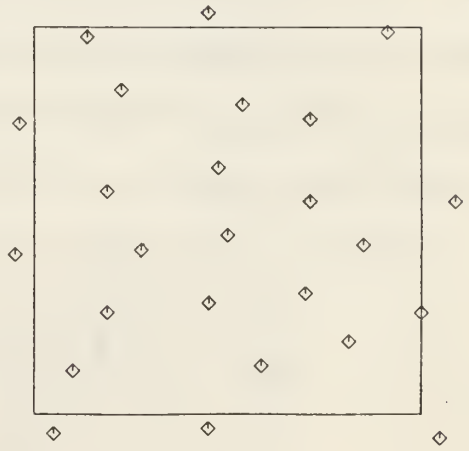

(c) Data Set 3

Figure 2.

of side 1/9 centered at (i/9,j/9), i, j = 0,1,...,9. These points are shown in Figure 2a.

Set 2: This set of 33 points was selected manually to have regions of varying density. These points are shown in Figure 2b.

Set 3: This set of 25 points was selected manually to yield a somewhat uniform coverage of the unit square, and are similar to a set appearing in [8]. These points are shown in Figure 2c.

The interpolants were evaluated on a uniform grid of 33 x 33 points in the unit square. The resulting surfaces are shown in Figures 3 and 4. Table 1 contains the maximum, mean, and RMS deviations at these points. For Method II a few of the display points lie outside the convex hull. For plotting purposes, these were set to zero and were omitted in the calculations leading to the errors of Table 1.

| Case | Max | Mean | RMS |
|---|---|---|---|
| I.1 | .0573 | .0079 | .0128 |
| I.2 | .1844 | .0340 | .0478 |
| I.3 | .1584 | .0353 | .0486 |
| II.1 | .0481 | .0072 | .0113 |
| II.2 | .1501 | .0326 | .0455 |
| II.3 | .1535 | .0349 | .0475 |

Table 1. Errors

Figures 3b and 4b show that both methods reproduce the surface quite well for data set 1. The main defect appears to be near the higher peak, particularly for Method I. As can be seen from the disposition of the points in Figure 2a, this is in a region where a relatively large gap between points occurs. A similar occurrence accounts for the depressed area behind the dip in both figures 3b and 4b.

Figures 3c and 4c are quite similar and both have noticeable defects when compared to the test surface. In particular, the dip is completely missed because the data points fail to define it. The appearance of a crease in Figure 4c near the right rear edge is due to the occurrence of a long thin triangle along that edge which causes blending of two nodal functions from points relatively far apart in the definition of the interpolant for that triangle. When these two nodal functions differ significantly, as they do here, rapid variations can occur across the narrow part of the triangle.

Figures 3d and 4d appear to be less alike than they actually are because values outside the convex hull have been set to zero in Figure 4d. The most significant difference between the two is near the left rear edge, where Figure 3d shows the surface (apparently) dipping down rather rapidly, while Figure 4d shows a near crease similar to that in Figure 4c. Because of a data point near (.47, .78), the dip is partially defined in this case, but since there are no other nearby points it is extended over a much wider area than in the test surface.

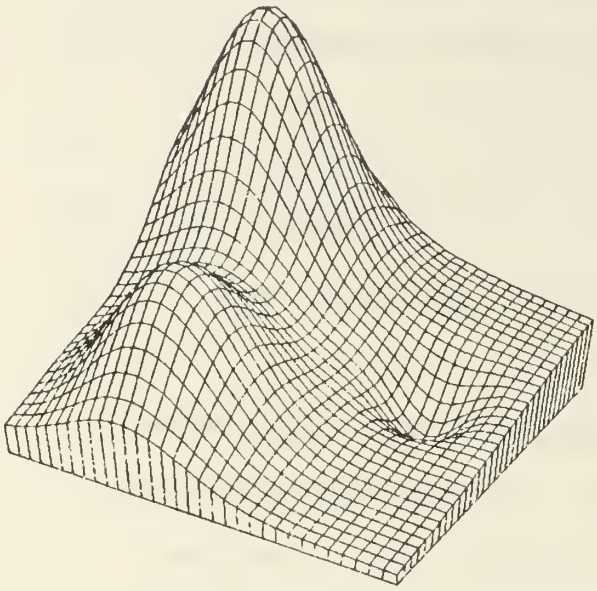

(a) Test surface

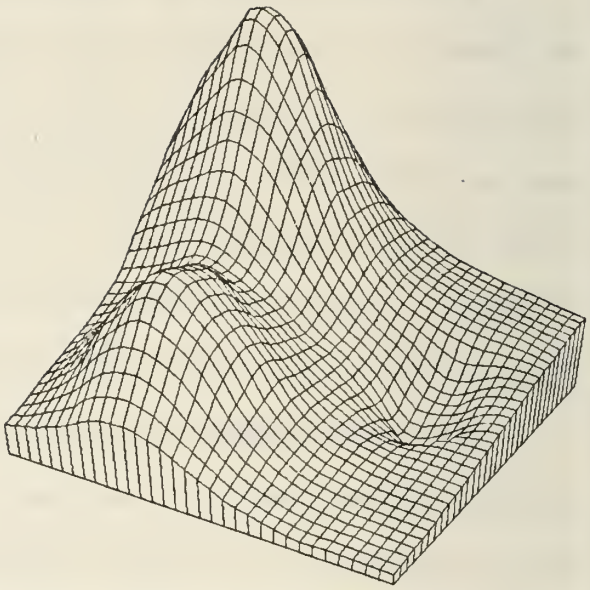

(b) Interpolant for Data Set 1

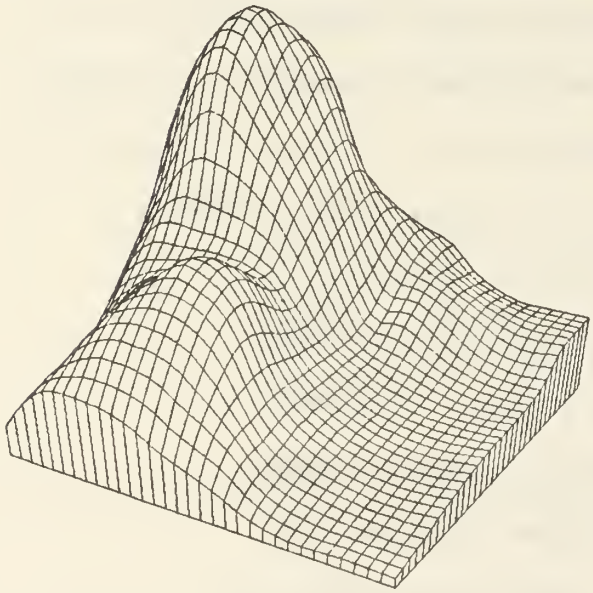

(c) Interpolant for Data Set 2

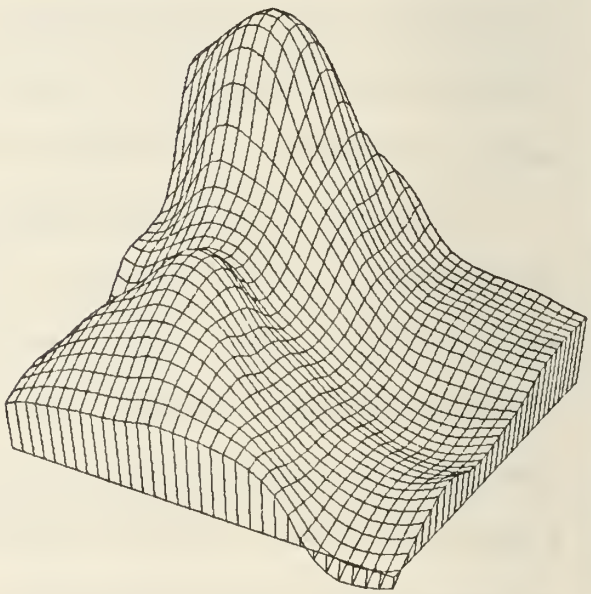

(d) Interpolant for Data Set 3

Figure 3: Method I

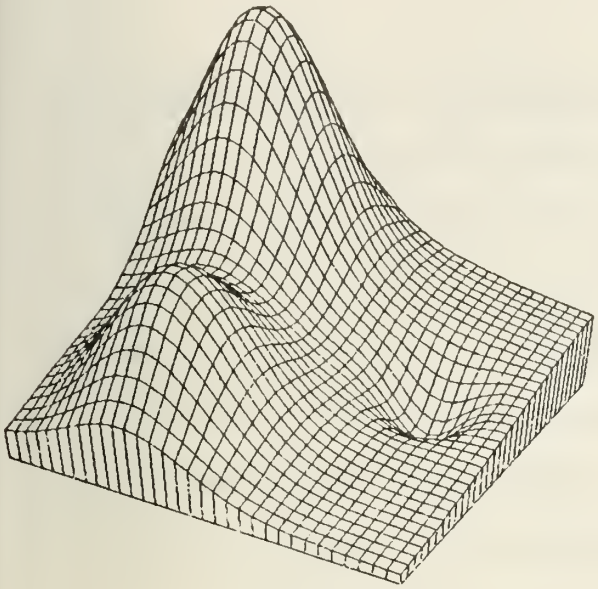

(a) Test surface

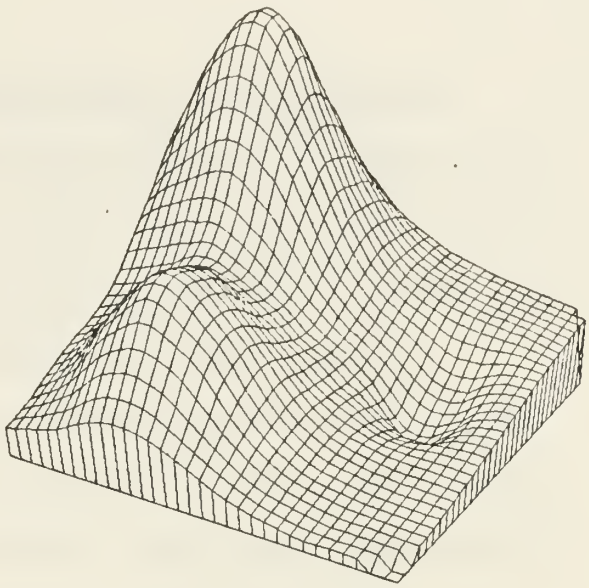

(b) Interpolant for Data Set 1

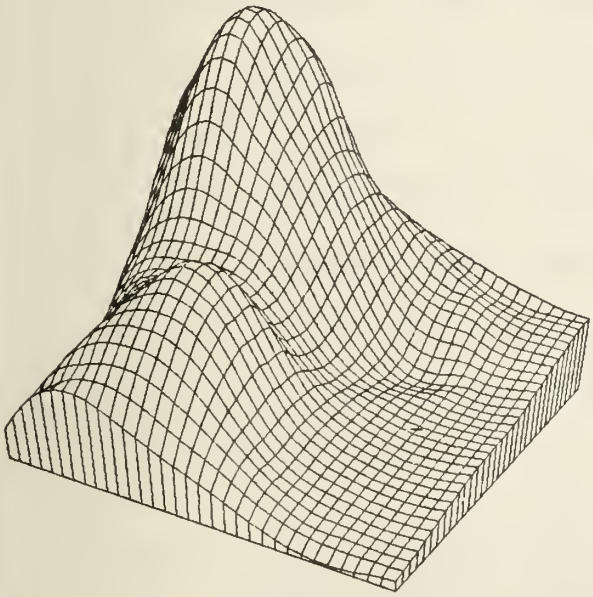

c) Interpolant for Data Set 2

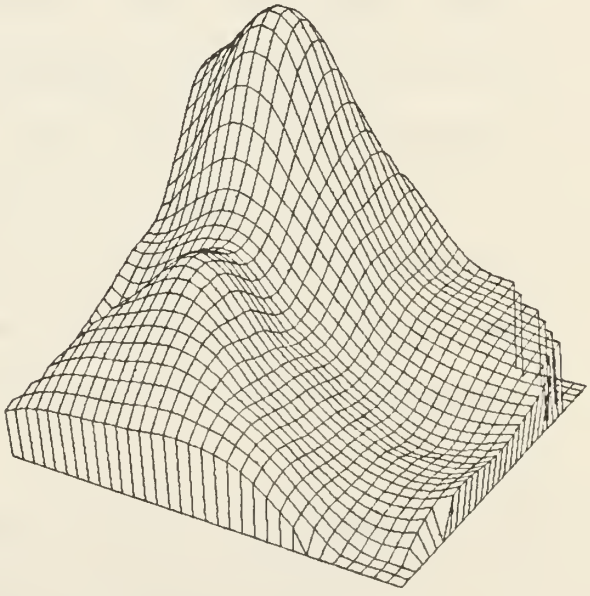

(d) Interpolant for Data Set 3

Figure 4: Method II

Another set of data obtained from Akima [1], which arises in a study of waveform distortion, is given in Table 2. We use this set to illustrate the effects of varying the parameters $N_q$ and $N_w$. The results are shown in Figure 5.

Figures 5a and 5c appear to be difficult to choose between. Very slight differences can be observed along the front edge. Figure 5e is definitely less desirable than 5a or 5c because of more undulations near the front edge and a higher peak at the right rear. Extensive testing has shown that Method I is fairly stable for values of $N_q$ and $N_w$ in the ranges given here.

Figure 5d appears to be the more desirable surface among 5b, 5d, and 5f. Figure 5b shows a small defect near the right front edge, while the choice between 5d and 5f is less obvious. All three show the characteristic defect over the long slim triangle at the right rear edge, allowing the surface to dip out of sight there. It should be pointed out that there is no known "parent" surface here, and in fact that behavior may be correct, although that part of the interpolant is not pleasing because of the very rapid changes which occur.

## 5. Conclusions and Recommendations

The two schemes discussed here have been found to be capable of generating reasonable interpolation functions in a variety of cases. A number of comments are appropriate, however.

First, we have restricted ourselves here to the discussion of local interpolants. Local methods are necessary for very large sets of data, but in exploring their properties

| i | $x_i$ | $y_i$ | $z_i$ | i | $x_i$ | $y_i$ | $z_i$ |
|---|---|---|---|---|---|---|---|
| 1 | 11.16 | 1.24 | 22.15 | 26 | 3.22 | 16.78 | 39.93 |
| 2 | 24.20 | 16.23 | 2.83 | 27 | 0.00 | 0.00 | 58.20 |
| 3 | 12.85 | 3.06 | 22.11 | 28 | 9.66 | 20.00 | 4.73 |
| 4 | 19.85 | 10.72 | 7.97 | 29 | 2.56 | 3.02 | 50.55 |
| 5 | 10.35 | 4.11 | 22.33 | 30 | 5.22 | 14.66 | 40.36 |
| 6 | 24.67 | 2.40 | 10.25 | 31 | 11.77 | 10.47 | 13.62 |
| 7 | 19.72 | 1.39 | 16.83 | 32 | 17.25 | 19.57 | 6.43 |
| 8 | 15.91 | 7.74 | 15.30 | 33 | 15.10 | 17.19 | 12.57 |
| 9 | 0.00 | 20.00 | 34.60 | 34 | 25.00 | 3.87 | 8.74 |
| 10 | 20.87 | 20.00 | 5.74 | 35 | 12.13 | 10.79 | 13.71 |
| 11 | 6.71 | 6.27 | 30.97 | 36 | 25.00 | 0.00 | 12.00 |
| 12 | 3.45 | 12.78 | 41.24 | 37 | 22.33 | 6.21 | 10.25 |
| 13 | 19.99 | 4.62 | 14.72 | 38 | 11.52 | 8.53 | 15.74 |
| 14 | 14.26 | 17.87 | 10.74 | 39 | 14.59 | 8.71 | 14.81 |
| 15 | 10.28 | 15.16 | 21.59 | 40 | 15.20 | 0.00 | 21.60 |
| 16 | 4.51 | 20.00 | 15.61 | 41 | 7.54 | 10.69 | 19.31 |
| 17 | 17.43 | 3.46 | 18.60 | 42 | 5.23 | 10.72 | 26.50 |
| 18 | 22.80 | 12.39 | 5.47 | 43 | 17.32 | 13.78 | 12.11 |
| 19 | 0.00 | 4.48 | 61.77 | 44 | 2.14 | 15.03 | 53.10 |
| 20 | 7.58 | 1.98 | 29.87 | 45 | 0.51 | 8.37 | 49.43 |
| 21 | 16.70 | 19.65 | 6.31 | 46 | 22.69 | 19.63 | 3.25 |
| 22 | 6.08 | 4.58 | 35.74 | 47 | 25.00 | 20.00 | 0.60 |
| 23 | 1.99 | 5.60 | 51.81 | 48 | 5.47 | 17.13 | 28.63 |
| 24 | 25.00 | 11.87 | 4.40 | 49 | 21.67 | 14.36 | 5.52 |
| 25 | 14.90 | 3.12 | 21.70 | 50 | 3.31 | 0.13 | 44.08 |

Table 2.

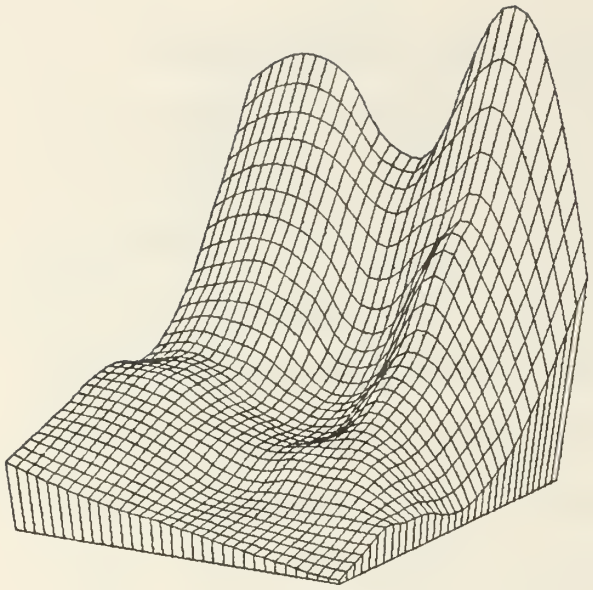

(a) Method I: $N_q$=12,$N_w$=6

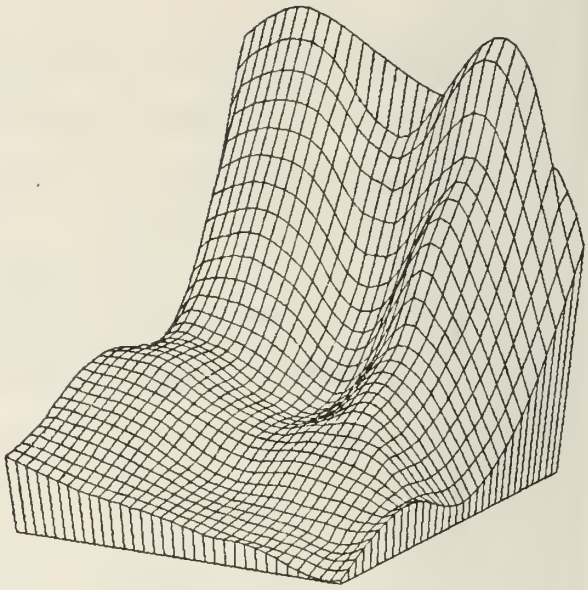

(b) Method II: $N_q$=12

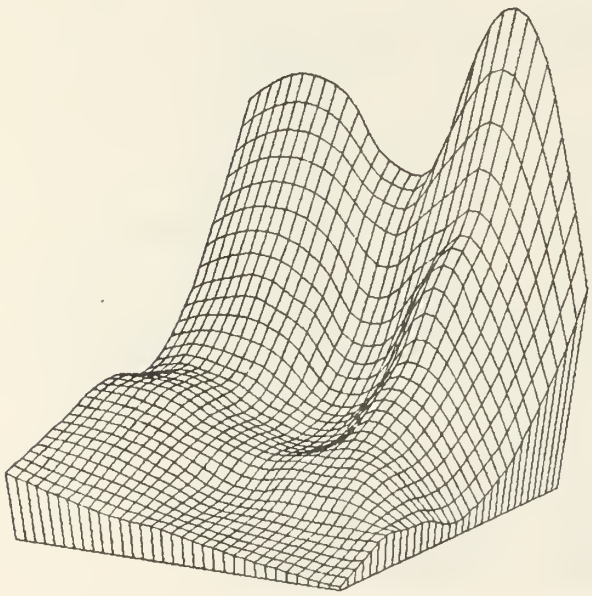

(c) Method I: $N_q$=18, $N_w$=9

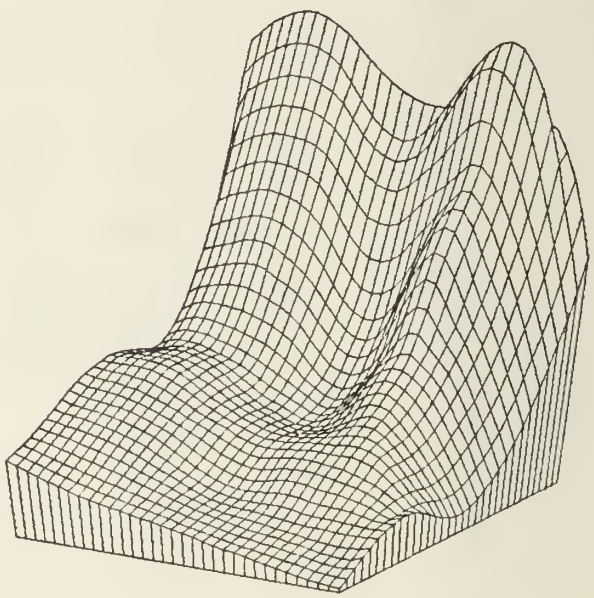

(d) Method II: $N_q$=18

Figure 5.

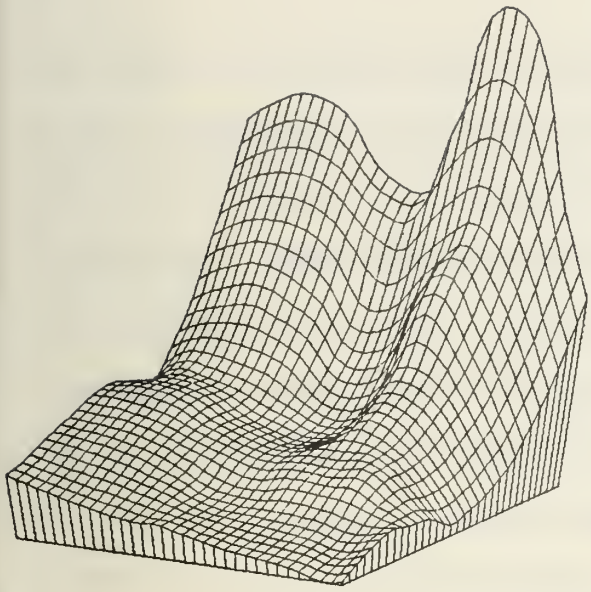

(e) Method I: $N_q$=24,$N_w$=12

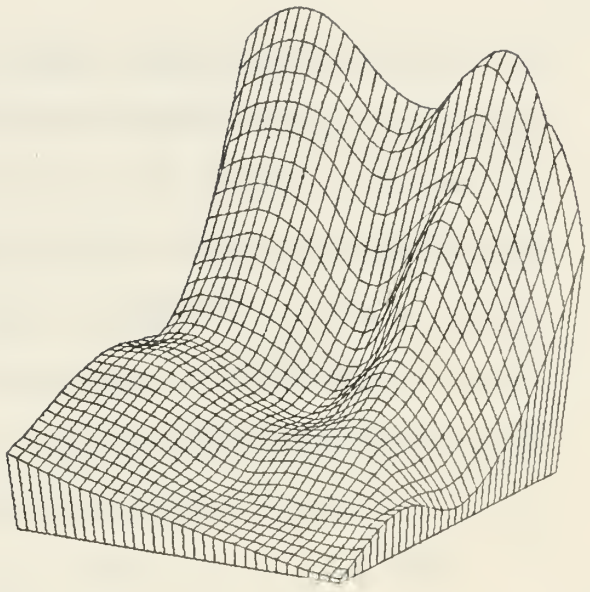

(f) Method II: $N_q$=24

Figure 5. (continued)

one need not consider large sets because they are local. We have only considered interpolation methods here, although we recognize that often it may be more appropriate to use approximation methods which smooth the data in some sense. While we have not investigated this possibility, it is clear that replacement of the nodal functions $Q_k(x,y)$ with local smoothing functions rather than ones which take on the value $f_k$ will lead to a smoothing approximation which is local.

The use of the same radius of influence for each point, and the calculation of that radius from the diameter of the point set is strictly a matter of convenience for the user. One could argue that this device makes the methods global since addition of a point will change the radius of influence and hence the entire interpolant. For this reason we made the computation of the radius of influence an option (although it is the default option). The use of different radii of influence could be a necessary and desirable feature when the density of points varies drastically over the point set. Our experience indicates that one should probably choose radii so that the disks associated with a point contain approximately 18 points for defining the nodal functions (Methods I and II) and about 9 points for defining the weight functions (Method I).

Regarding the choice between Method I and Method II, we make the following comments: Method I has the advantage of simplicity. While Method II requires a triangulation (and the machinery for generating it if it is not already available),

and thus more auxiliary storage, it is considerably faster since each evaluation involves only three nodal functions, while Method I typically involves about 9 ($N_w = 9$) nodal functions. Method II also has the disadvantages noted in the examples when long thin triangles occur. Method II is not readily extended to more than two independent variables, as is Method I. Nonetheless, for certain applications, Method II may be the appropriate choice, particularly if a triangulation is already in existence.

In conclusion, we note that all local methods involve some ad hoc assumptions and/or parameters to be specified by the user. The methods we propose have endured through extensive testing of their fitting properties and appropriate values for their parameters. We feel they will perform quite adequately in a variety of situations. Nonetheless, we recognize that selection of a suitable interpolant is a subjective matter even in the case of one independent variable, and thus the choice of an interpolant ultimately rests with the user.

FORTRAN programs which implement Methods I and II are available on request from the authors.

Acknowledgement: We wish to thank William J. Gordon for encouragement and helpful criticism during the preparation of this paper.

## References


1. Akima, H., "A method of bivariate interpolation and smooth surface fitting for irregularly distributed data points," ACM TOMS 4(1978) 144-159, and "Algorithm 526: Bivariate interpolation and smooth fitting for irregularly distributed data points," ACM TOMS 4(1978) 160-164.

2. Barnhill, R. E., "Representation and approximation of surfaces," in Mathematical Software III, John R. Rice, ed., Academic Press, New York, 1977, pp. 69-120.

3. Franke, R., "Locally determined smooth interpolation at irregularly spaced points in several variables," JIMA 19(1977) 471-482.

4. Franke, R., "A critical comparison of some methods for interpolation of scattered data," Naval Postgraduate School Technical Report, NPS53-79-003, 1979.

5. Gordon, W. J. and Wixom, J., "On Shepard's method of metric interpolation to bivariate and multivariate data," Mathematics of Computation 32(1978) 253-264.

6. Lawson, C. L., "Software for $C^1$ surface interpolation," in Mathematical Software III, John R. Rice, ed., Academic Press, New York, 1977, pp. 161-194.

7. McLain, D. H., "Drawing contours from arbitrary data points," The Computer Journal, 17(1974) 318-324.

8. McLain, D. H., "Two dimensional interpolation from random data," The Computer Journal 19, (1976) 178-181, and Errata, The Computer Journal 19, (1976) 384.

9. Nielson, G., "Minimum norm interpolation in triangles," To appear in SIAM Journal on Numerical Analysis.

10. Schumaker, L. L., "Fitting surfaces to scattered data," in Approximation Theory II, edited by G. G. Lorentz, C. K. Chui, and L. L. Schumaker, Academic Press, 1976, pp. 203-268.

11. Shepard, D., "A two dimensional interpolation function for irregularly spaced data," Proc. 23rd Nat. Conf. ACM (1968) 517-523.

DISTRIBUTION LIST

| | |
|---|---|
| Defense Technical Information Center<br>Cameron Station<br>Alexandria, VA 22314 | 2 |
| Dudley Knox Library<br>Naval Postgraduate School<br>Monterey, CA 93940 | 2 |
| Dean of Research<br>Naval Postgraduate School<br>Monterey, CA 93940 | 2 |
| Department of Mathematics<br>C. O. Wilde, Chairman<br>F. D. Faulkner, Acting Chairman<br>Professor A. Schoenstadt<br>Professor R. Franke<br>Naval Postgraduate School<br>Monterey, CA 93940 | <br>1<br>1<br>1<br>10 |
| Dr. Richard Lau<br>Office of Naval Research<br>1030 East Green St.<br>Pasadena, CA 91106 | 1 |
| Professor R. E. Barnhill<br>Department of Mathematics<br>University of Utah<br>Salt Lake City, UT 84112 | 1 |
| Professor G. M. Nielson<br>Department of Mathematics<br>Arizona State University<br>Tempe, AZ 85281 | 10 |
| Chief of Naval Research<br>ATT: Mathematics Program<br>Arlington, VA 22217 | 2 |
| Rosemary E. Chang<br>Sandia Laboratories<br>Applied Mathematics, Division 2-8235<br>Livermore, CA 94550 | 1 |
| Hiroshi Akima<br>Office of Telecommunications<br>Department of Commerce<br>Boulder, CO 80302 | 1 |

Director
Naval Research Laboratory
Department of the Navy
4555 Overlook Avenue, S.W.
Washington, D.C. 20375
ATTN: Tech. Information Officer — 6

Director
Office of Naval Research/Branch Office
495 Summer Street
Boston, MA 02210 — 1

Office of Naval Research
New York Area Office
715 Broadway - 5th floor
New York, NY 10003 — 1

Director
Office of Naval Research/Branch Office
536 South Clark Street
Chicago, IL 60605 — 1

Office of Naval Research
San Francisco Area Office
760 Market Street - Room 447
San Francisco, CA 94102 — 1

Director
Naval Research Laboratory
Library, Code 2620
4555 Overlook Avenue, S.W.
Washington, D.C. 20375 — 6

Stanford University
Department of Mathematics
Stanford, CA 94305 — 1

Courant Institute of
Mathematical Sciences
New York University
New York, NY 10012 — 1

Massachusetts Institute of Technology
Department of Mathematics
Cambridge, MA 02139 — 1

Dr. J. A. DeSanto
Naval Research Laboratory
Code 8340
Washington, D.C. 20375 — 1

Dr. Larry Stedman
Naval Ship Research and
Development Center
Code 1850
Bethesda, MD 20034 1

Dr. Thomas Corin
Naval Ship Research and
Development Center
Code 1850
Bethesda, MD 20034 1

Dr. Robert Buchal
Naval Research Laboratory
Acoustic Environmental Support
Detachment
Washington, D.C. 20375 1

Dr. J. W. Enig
Naval Surface Weapons Center
Mathematics Department
White Oak
Silver Spring, MD 20910 1

Dr. Bruce J. McDonald
Office of Naval Research
Code 436, Room 607
Arlington, VA 22217 1

Mr. Allen L. Hankinson
Naval Ship Research and
Development Center
Code 1833
Bethesda, MD 20034 1

Charles Micchelli
Thomas J. Watson Research Center
P. O. Box 218
Yorktown Heights, NY 10598 1

Michael Minkoff
Applied Mathematics Division
Argonne National Laboratory
9700 South Cass Avenue
Argonne, IL 60439 1

R. K. Rew
NCAR
P. O. Box 3000
Boulder, CO 80307 1

W. Fichtner
Bell Laboratories
Murray Hill, NJ 07974 1

Peter R. Eiseman 1
ICASE
MS 132C
NASA Langley Research Center
Hampton, VA 23665

Stephen C. Banks 1
Sun Production Co.
503 N. Central Expressway
Richardson, TX 75080

Pablo Barrera 1
Facultao de Ciencias
Dept. de Matematicas
U. N. A. M.
Mexico 20, D. F.
MEXICO

Richard A. Hansen 1
308 TMCB
Brigham Young University
Provo, UT 84601

P. H. Merz 1
Chevron Research Co.
P. O. Box 1627
Richmond, CA 94802

C. Birch 1
P. O. Box 1267
Conoco R & D
Ponca City, OK 74601

James Lyness 1
AMD-ANL
Argonne, IL 60439

Fred N. Fritsch 1
Lawrence Livermore Laboratories
P. O. Box 808 (L-300)
Livermore, CA 94500

W. J. Schaffers 1
Dupont Co., Engineering Department
Exp. Station, 304
Wilmington, DE 19898

U. Ascher 1
Department of Computer Science
University of British Columbia
Vancouver, BC, CANADA

Joe McGrath
KMS Fusion, Inc.
3941 Research Park Dr.
Ann Arbor, MI 48104 1

P. S. Jensen
Lockheed Research 5233/205
3251 Hanover St.
Palo Alto, CA 94304 1

Myron Ginsberg
Computer Science Department
General Motors Research Laboratory
Warren, MI 48090 1

L. Kratz
Mathematics Department
Idaho State University
Pocatello, ID 83209 1

Alan Pierce
Amoco Production Co.
P. O. Box 591
Tulsa, OK 74102 1

A. K. Cline
Department of Computer Science
University of Texas at Austin
Austin, TX 78712 1

W. Roy Wessel
CDC
7995 E. Prentice Ave.
Englewood, CO 80111 1

J. W. Chalmers
HAO/NCAR
Box 3000
Boulder, CO 80307 1

Richard B. Evans
Ocean Data Systems, Inc.
6000 Executive Blvd.
Rockville, MD 20852 1

L. H. Seitelman
Pratt and Whitney Aircraft
400 Main Street
East Hartford, CT 06108 1

John A. Carpenter
Oak Ridge National Laboratories
Bldg. 4500-N
Room E208
P. O. Box X
Oak Ridge, TN 37830 1